Reviews

Matrix Preparation and Spectroscopic and Theoretical Investigations of Simple Methylidene and Methylidyne Complexes of Group 4−6 Transition Metals

Lester Andrews*

Department of Chemistry, University of Virginia, P.O. Box 400319, Charlottesville, Virginia 22904-4319

Han-Gook Cho

Department of Chemistry, University of Incheon, 177 Dohwa-dong, Nam-ku, Incheon 402-749, South Korea

Received April 9, 2006

A new generation of simple methylidene complexes has been prepared by reactions of excited group 4−6 transition metal atoms with methyl halides and methane in solid argon. These $CH_2{=}MHX$ (X = F, Cl, Br, I) and $CH_2{=}MH_2$ methylidene complexes exhibit agostic bonding effects of CH_2 and MH_2 distortion. The reactions proceed through the $CH_3{-}MX$ insertion product followed by α-H transfer on an excited potential energy surface. The higher valence of group 6 metals sustains a second α-H transfer to form the $CH{\equiv}MH_2X$ (M = Mo, W, X = H, F, Cl, Br) methylidyne complexes, and electron capture by group 5 $CH_2{=}MHX$ (M = Nb, Ta, X = H, F, Cl, Br) methylidene complexes gives rise to the analogous $CH{\equiv}MH_2X^-$ methylidyne anion complexes. These simple organometallic complexes are identified by matrix infrared spectra through isotopic substitution and by comparison with vibrational characteristics calculated by DFT. Periodic trends in agostic interactions are illustrated for different metals and halogen substituents. Complementary investigations for group 3 and for group 7−9 transition metals and for early lanthanide and actinide metals are also discussed and compared.

Introduction

High-oxidation-state alkylidene ($M{=}CR_1R_2$) and alkylidyne ($M{\equiv}CR$) complexes have been investigated extensively over the last three decades, and many of these complexes reveal agostic bonding.[1] This large body of work has provided a wealth of information on the nature of metal coordination chemistry and important new compounds for application as metathesis and polymerization catalysts for alkenes and alkynes.[1−5] Such ligand-stabilized compounds are synthesized by intramolecular α-H transfer from a bis(alkyl) precursor. Agostic bonding in these systems involves an α-H-to-metal interaction and stabilization of the C=M double bond,[6−10] and simple methylidene model systems made from methyl halides and methane can help to understand this bonding interaction through detailed quantum-chemical calculations.

Early theoretical studies of simple group 4 $CH_2{=}MH_2$ methylidene complexes employed minimum or small basis sets and reported symmetrical planar structures.[11,12] More recent MC/LMO/CI calculations still employed a small basis for carbon without polarization functions, assumed C_{2v} structures, and determined them to be stable.[13] Later MCSCF calculations for $CH_2{=}TiH_2$ found the symmetrical planar structure to be more stable than a symmetrical twisted structure.[14] To be practical, multireference calculations require the imposition of symmetry.

Recently, density functional theory (DFT) has been employed to investigate agostic interactions in too many complexes to list here (for examples and reviews see refs 7, 9, 10, and 15−17), and the importance of polarization functions on carbon has been noted.[7,9] This was substantiated in subsequent calculations

* To whom correspondence should be addressed. E-mail: lsa@virginia.edu.

(1) Schrock, R. R. *Chem. Rev.* **2002**, *102*, 145.
(2) Crabtree, R. H. *Chem. Rev.* **1995**, *95*, 987 and references therein.
(3) Grubbs, R. H.; Coates, G. W. *Acc. Chem. Res.* **1996**, *29*, 85.
(4) (a) Tran, E.; Legzdins, P. *J. Am. Chem. Soc.* **1997**, *119*, 5071. (b) Choi, S.-H.; Lin, Z. *Organometallics* **1999**, *18*, 5488.
(5) Buchmeiser, M. R. *Chem. Rev.* **2000**, *100*, 1565.
(6) Brookhart, M.; Green, M. L. H. *J. Organomet. Chem.* **1983**, *250*, 395.
(7) Ujaque, G.; Cooper, A. C.; Maseras, F.; Eisenstein, O.; Caulton, K. G. *J. Am. Chem. Soc.* **1998**, *120*, 361.
(8) Wada, K.; Craig, B.; Pamplin, C. B.; Legzdins, P.; Patrick, B. O.; Tsyba, I.; Bau, R. *J. Am. Chem. Soc.* **2003**, *125*, 7035.
(9) Clot, E.; Eisenstein, O. Agostic Interactions from a Computational Perspective. In *Structure and Bonding, Computational Inorganic Chemistry*; Kaltzoyannis, N., McGrady, E., Eds.; Springer-Verlag: Heidelberg, Germany, 2004; pp 1−36.
(10) Scherer, W.; McGrady, G. S. *Angew. Chem., Int. Ed.* **2004**, *43*, 1782.
(11) Franci, M. M.; Pietro, W. J.; Hout, R. F., Jr.; Hehre, W. J. *Organometallics* **1983**, *2*, 281, 815.
(12) Dobbs, K. D.; Hehre, W. J. *J. Am. Chem. Soc.* **1986**, *108*, 4663.
(13) Cundari, T. R.; Gordon, M. S. *J. Am. Chem. Soc.* **1992**, *114*, 539.
(14) Chung, G.; Gordon, M. S. *Organometallics* **2003**, *22*, 42.
(15) Haaland, A.; Scherer, W.; Rudd, K.; McGrady, G. S.; Downs, A. J.; Swang. O. *J. Am. Chem. Soc.* **1998**, *120*, 3762.
(16) Agapie, T.; Diaconescu, P. L.; Cummins, C. C. *J. Am. Chem. Soc.* **2002**, *124*, 2412.
(17) van der Boom, M. E.; Iron, M. A.; Atasoylu, O.; Shimon, L. J. W.; Rozenberg, H.; Ben-David, Y.; Konstantinovski, L.; Martin, J. M. L.; Milstein, D. *Inorg. Chim. Acta* **2004**, *357*, 1854.

10.1021/om060318l CCC: $33.50
Publication on Web 07/22/2006

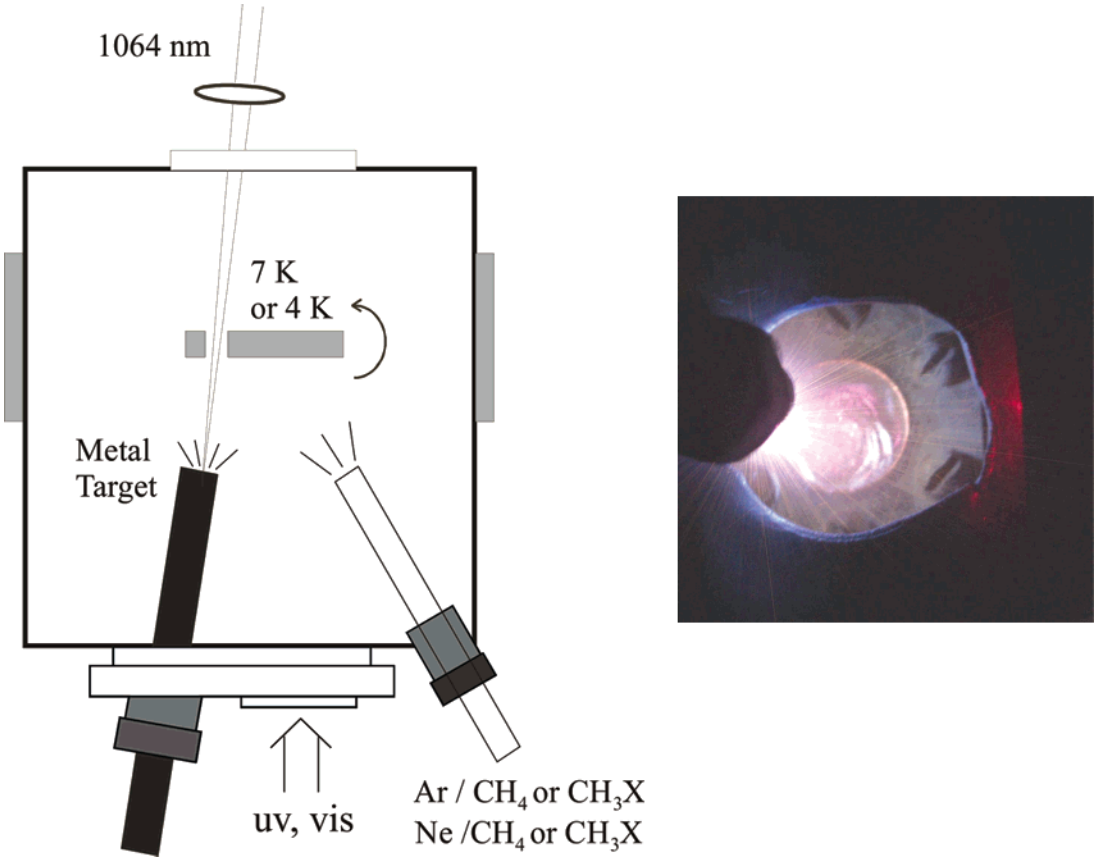

Figure 1. (left) Schematic diagram of laser-ablation matrix-isolation apparatus for reacting transition-metal atoms and methane or methyl halides and trapping the products in solid argon or neon for infrared spectroscopic and photochemical investigations. (right) Photograph of laser-ablation process where zirconium atoms are codeposited onto the 7 K cesium iodide window along with argon/reagent sample. The Zr rod is on the left side, and the cold sample window is in the center. Note the 4-40 machine screw heads on the copper mount with 0.50 in. diameter cutout to expose the sample window. Photograph taken through UV, vis irradiation port. (Photograph courtesy of A. B. Baker.)

on $CH_2{=}ZrH_2$ from this laboratory.[18] Very recently, numerous theoretical methods from HF to CCSD(T) and including DFT have been used to evaluate the agostic bond in the simple model complex $CH_2{=}TiHF$.[19] Further, this group has calculated the compliance matrix for different agostic complexes and estimated the agostic bond strength to be in the range of a typical hydrogen bond.[19]

Methane activation experiments have been performed previously with excited metal atoms. Group 2 and 12 (s^2) metal atoms in the ^3P excited state inserted to form the $CH_3{-}MH$ species with linear C−M−H structures.[20,21] In fact, simple Grignard reagent molecules $CH_3{-}MgX$ (X = F, Cl, Br, I) were produced from excited Mg atoms and methyl halides.[22] Aluminum was the first metal atom observed to activate methane without photoexcitation.[23] Moving on to transition-metal atoms, very early work found atomic V to be unreactive in solid methane.[24] Later studies of first-row transition-metal atoms subjected to UV photoexcitation in pure solid methane formed a single product identified as $CH_3{-}MH$ for M = Mn, Fe, Co, Cu, Zn, but Ca, Ti, and Cr failed to react under the conditions of these experiments.[23,25] Although Ti did not activate neat solid methane at 10 K, Zr reacted with solid isobutane and neopentane at 77 K.[23,26] In contrast, previous thermal transition-metal atom work has shown that only Rh is reactive without photoexcitation, and very recently ground-state rhodium atoms have been found to activate methane in solid argon to form $CH_3{-}RhH$, which was predicted theoretically to be a stable molecule.[27−29] Finally, these pioneering investigations with transition-metal atoms and methane reported no evidence for methylidene complexes.

In this review article, we will present an overview of recent matrix-isolation infrared experimental and density functional theoretical investigations of simple early-transition-metal $CH_2{=}MHX$ methylidene and $CH{\equiv}MH_2X$ methylidyne complexes mostly from groups 4−6.[18,30−43] We also describe some complementary results with group 3 and group 7−9 transition metals, aimed at exploring the limit of α-H transfer in $CH_3{-}MH$ complexes,[44] and the evolution of this work to the early lanthanide[45] and actinide metals.[46−49] We will emphasize periodic trends in metal centers and halide substituent effects that help to characterize the widely investigated agostic interaction in methylidene complexes.

Experimental and Computational Methods

The essential elements of our matrix-isolation laser-ablation apparatus shown in Figure 1 have been described in more detail

(18) Cho, H.-G.; Wang, X.; Andrews, L. *J. Am. Chem. Soc*. **2005**, *127*, 465 (Zr + CH_4).
(19) von Frantzius, G.; Streubel, R.; Brandhorst, K.; Grunenberg, J. *Organometallics* **2006**, *25*, 118.
(20) Greene, T. M.; Lanzisera, D. V.; Andrews, L.; Downs, A. J. *J. Am. Chem. Soc*. **1998**, *120*, 6097.
(21) Greene, T. M.; Andrews, L.; Downs, A. J. *J. Am. Chem. Soc*. **1995**, *117*, 8180 (group 12 + CH_4).
(22) Bare, W. D.; Andrews, L. *J. Am. Chem. Soc*. **1998**, *120*, 7293.
(23) Klabunde, K. J.; Tanaka. Y. *J. Am. Chem. Soc*. **1983**, *105*, 3544.
(24) Klotzbucher, W. E.; Mitchell, S. A.; Ozin, G. A. *Inorg. Chem.* **1977**, *16*, 3063.
(25) (a) Billups, W. E.; Konarski, M. M.; Hauge, R. H.; Margrave, J. L. *J. Am. Chem. Soc*. **1980**, *102*, 7393. (b) Ozin, G. A.; McIntosh, D. F.; Mitchell, S. A.; Garcia-Prieto, J. *J. Am. Chem. Soc*. **1981**, *103*, 1574.

previously.[50,51] A focused, pulsed Nd-YAG laser (5−20 mJ/pulse, 10 Hz) ablates transition-metal atoms toward the cryogenically cooled window (4 K for neon or 7 K for argon matrix experiments) for codeposition and reaction with Ne/CH_4, Ne/CH_3X, Ar/CH_4, and Ar/CH_3X host matrix/reagent gas mixtures. The photograph illustrates the emission plume from a Zr metal target in front of the cold sample window during the laser ablation and sample codeposition process. Isotopically enriched (^{13}C, D) reagents were also employed. Infrared spectra were recorded by Nicolet Fourier transform instruments at 0.5 cm^{-1} resolution and 0.1 cm^{-1} frequency accuracy after deposition, after subsequent irradiation by a mercury arc street lamp (Sylvania, 175 W, outer globe removed) in combination with glass filters and after sequential annealing of the matrix sample.

Supporting quantum-chemical structure, energy, and vibrational frequency calculations were done using the G98 and G03 program systems, the B3LYP density functional, the medium 6-311++G(2d,p) or the large 6-311++G(3df,3pd) Gaussian basis set for C and H atoms, and the SDD effective core potential and basis for transition-metal atoms.[52−55] To substantiate the use of DFT for the C═M systems, the more rigorous and time-consuming CCSD and CCSD-(T) methods were also employed for comparison.[56]

The simple new methylidene complexes CH_2═MHX to be reviewed here were identified by matrix infrared spectroscopy through isotopic substitution and matching of isotopic frequencies computed by DFT. In this review the major isotopic frequencies will be discussed, and the reader can find other isotopic frequency counterparts in our original papers. Likewise, calculated frequencies will be given for one example, and the reader can compare the calculated frequencies for other subject molecules in our referenced work.

Group 3

Reactions of group 3 metal atoms with methyl halides and methane were investigated after groups 4−6 in order to characterize α-H transfer to the most electron-deficient transition metals, but in keeping with the periodic table order, group 3 metal systems will be examined first. We quickly discovered that C−X bond activation in methyl halides leads to a higher product yield than C−H bond activation in methane; therefore, Y and CH_3F results will be discussed here in part for comparison with subsequent transition-metal atoms.[44] The flagship new product absorption at 1397.7 cm^{-1} on codeposition of laser-ablated Y atoms and CH_3F is doubled in intensity by UV irradiation. This band shifts to 1000.5 cm^{-1} with CD_3F, and the H/D isotopic frequency ratio (1.3970) is appropriate for a Y−H stretching mode. Two other associated absorptions at 575.1 and 503.4 cm^{-1} are due to primarily Y−F and C−Y stretching modes, based on carbon-13 shifts, and the CH_2−YHF product is thereby identified. The three strongest absorptions in the infrared spectrum are predicted by B3LYP calculations at 1445, 596, and 507 cm^{-1}, which are in excellent agreement and show the deviations expected for this level of theory.[57,58]

The structure calculated for CH_2−YHF illustrated in Figure 2 is almost planar, with very slight differences in the C−H bond lengths and H−C−Y angles and a long C−Y bond length of 2.331 Å. However, this is slightly shorter than the 2.390 Å value computed for CH_3−YF; therefore, we conclude that the C−Y bond has a small amount of π character, but there is no evidence for agostic distortion in the CH_2 subgroup. This CH_2−YHF radical needs another electron to form the classical methylidene complex (CH_2═ZrHF).

A weak 561 cm^{-1} band decreases on UV irradiation and is in agreement with the strongest absorption (by a factor of 10) predicted for CH_3−YF at 562 cm^{-1}. The Y−F stretching modes observed here fall below the 631.4 cm^{-1} value for YF itself.[59] On UV irradiation α-H transfer in CH_3−YF gives rise to the strong Y−H stretching mode at 1397.7 cm^{-1}.

The analogous CH_2−YHCl and CH_2−YHBr complexes with strong absorptions at 1419.6 and 1424.1 cm^{-1}, respectively, have

(26) Remick, R. J.; Asunta, T. A.; Skell, P. S. *J. Am. Chem. Soc.* **1979**, *101*, 1320.
(27) Klabunde, K. J.; Jeong, G. H.; Olsen, A. W. In *Selective Hydrocarbon Activation: Principles and Progress*; Davies, J. A., Watson, P. L., Greenberg, A., Liebman, J. F., Eds.; VCH: New York, 1990; pp 433−466.
(28) Wang, G.; Chen, M.; Zhou, M. *Chem. Phys. Lett.* **2005**, *412*, 46.
(29) Bloomberg, M. R. A.; Siegbahn, P. E. M.; Svensson, M. *J. Am. Chem. Soc.* **1992**, *114*, 6095.
(30) (a) Cho, H.-G.; Andrews, L. *J. Phys. Chem. A* **2004**, 108, 6294. (b) Cho, H.-G.; Andrews, L. *Inorg.* Chem. **2004**, *43*, 5253 (Ti + CH_3F).
(31) Andrews, L.; Cho, H.-G.; Wang, X. *Inorg. Chem.* **2005**, *44*, 4834 (Ti + CH_4).
(32) Cho, H.-G.; Andrews, L. *J. Am. Chem. Soc.* **2004**, *126*, 10485 (Zr + CH_3F).
(33) Andrews, L.; Cho, H.-G.; Wang, X. *Angew. Chem., Int. Ed.* **2005**, *44*, 113 (Zr + CH_4).
(34) Cho, H.-G.; Andrews, L. *Organometallics* **2004**, *23*, 4357 (Hf + CH_3F).
(35) Cho, H.-G.; Wang, X.; Andrews, L. *Organometallics* **2005**, *24*, 2854 (Hf + CH_4).
(36) Cho, H.-G.; Andrews, L. *Inorg. Chem.* **2005**, *44*, 979 (Ti + CH_3X).
(37) Cho, H.-G.; Andrews, L. *Chem. Eur. J.* **2005**, *11*, 5017 (Mo + CH_3F).
(38) Cho, H.-G.; Andrews, L. *J. Am. Chem. Soc.* **2005**, *127*, 8226 (Mo + CH_4).
(39) Cho, H.-G.; Andrews, L. *Organometallics* **2005**, *24*, 5678 (Cr and W + CH_3F).
(40) Cho, H.-G.; Andrews, L.; Marsden, C. *Inorg. Chem.* **2005**, *44*, 7634 (W + CH_4).
(41) Cho, H.-G.; Andrews, L. *Organometallics* **2006**, *25*, 477 (Nb + CH_3F).
(42) Cho, H.-G.; Andrews, L. *J. Phys. Chem. A* **2006**, *110*, 3886. (V, Nb, and Ta + CH_4).
(43) Cho, H.-G.; Kim, T.-H.; Andrews, L. *Chem. Asian J.*, in press (Zr, Hf + CH_3X).
(44) Cho, H.-G.; Andrews, L. Unpublished results, 2006 (group 3 and 7−9 reactions).
(45) Lyon, J. T.; Cho, H.-G.; Andrews, L. Unpublished results, 2006 (lanthanide metal reactions with methane and methyl halides).
(46) Andrews, L.; Cho, H.-G. *J. Phys. Chem. A* **2005**, *109*, 6796.
(47) Lyon, J. T.; Andrews, L. *Inorg. Chem.* **2005**, *44*, 8610.
(48) Lyon, J. T.; Andrews, L. *Inorg. Chem.* **2006**, *45*, 1847.
(49) Lyon, J. T.; Andrews, L.; Wang, T.; Bursten, B. E.; Wisborg-Krogh, J.; Roos, B. O. To be submitted for publication.
(50) Andrews, L.; Citra, A. *Chem. Rev.* **2002**, *102*, 885 and references therein.
(51) Andrews, L. *Chem. Soc. Rev.* **2004**, *33*, 123 and references therein.
(52) Frisch, M. J.; Trucks, G. W.; Schlegel, H. B.; Scuseria, G. E.; Robb, M. A.; Cheeseman, J. R.; Montgomery, J. A., Jr.; Vreven, T.; Kudin, K. N.; Burant, J. C.; Millam, J. M.; Iyengar, S. S.; Tomasi, J.; Barone, V.; Mennucci, B.; Cossi, M.; Scalmani, G.; Rega, N.; Petersson, G. A.; Nakatsuji, H.; Hada, M.; Ehara, M.; Toyota, K.; Fukuda, R.; Hasegawa, J.; Ishida, M.; Nakajima, T.; Honda, Y.; Kitao, O.; Nakai, H.; Klene, M.; Li, X.; Knox, J. E.; Hratchian, H. P.; Cross, J. B.; Bakken, V.; Adamo, C.; Jaramillo, J.; Gomperts, R.; Stratmann, R. E.; Yazyev, O.; Austin, A. J.; Cammi, R.; Pomelli, C.; Ochterski, J. W.; Ayala, P. Y.; Morokuma, K.; Voth, G. A.; Salvador, P.; Dannenberg, J. J.; Zakrzewski, V. G.; Dapprich, S.; Daniels, A. D.; Strain, M. C.; Farkas, O.; Malick, D. K.; Rabuck, A. D.; Raghavachari, K.; Foresman, J. B.; Ortiz, J. V.; Cui, Q.; Baboul, A. G.; Clifford, S.; Cioslowski, J.; Stefanov, B. B.; Liu, G.; Liashenko, A.; Piskorz, P.; Komaromi, I.; Martin, R. L.; Fox, D. J.; Keith, T.; Al-Laham, M. A.; Peng, C. Y.; Nanayakkara, A.; Challacombe, M.; Gill, P. M. W.; Johnson, B.; Chen, W.; Wong, M. W.; Gonzalez, C.; Pople, J. A. *Gaussian 03*, revision B.04; Gaussian, Inc.: Wallingford, CT, 2003.
(53) (a) Becke, A. D. *J. Chem. Phys.* **1993**, *98*, 5648. (b) Lee, C.; Yang, Y.; Parr, R. G. *Phys. Rev. B* **1988**, *37*, 785.
(54) Frisch, M. J.; Pople, J. A.; Binkley, J. S. *J. Chem. Phys.* **1984**, *80*, 3265.
(55) Andrae, D.; Haeussermann, U.; Dolg, M.; Stoll, H.; Preuss, H. *Theor. Chim. Acta* **1990**, *77*, 123.
(56) Purvis, G. D.; Bartlett, R. J. *J. Chem. Phys.* **1982**, *76*, 1910.
(57) Scott, A. P.; Radom, L. *J. Phys. Chem.* **1996**, *100*, 16502.
(58) Andersson, M. P.; Uvdal, P. L. *J. Phys. Chem. A* **2005**, 109, 3937.
(59) Fischell, D.; Brayman, H. C.; Cool, T. A. *J. Chem. Phys.* **1980**, *73*, 4260.

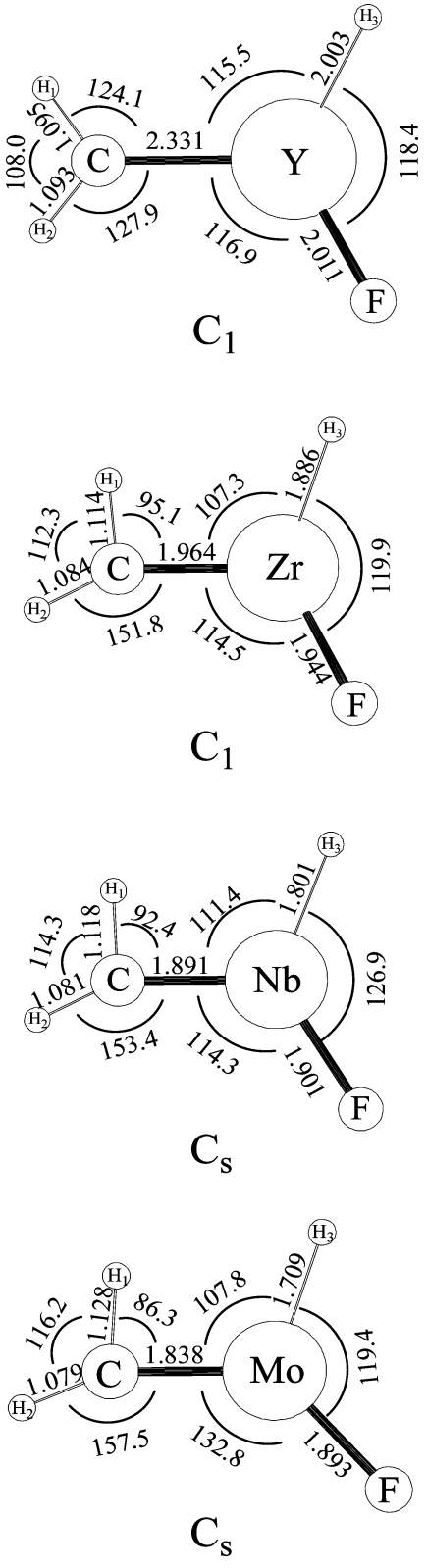

Figure 2. Structures of CH_2═MHF complexes (M = Y, Zr, Nb, Mo) calculated at the B3LYP/6-311++G(3df,3pd)/SDD (for metal) level of theory. Bond lengths are in angstroms and angles in degrees.

been prepared from CH_3Cl and CH_3Br.[44] Note that the Y−H stretching frequencies for the CH_2−YHX complexes increase with increasing halogen size. Finally, the CH_2−YHF and CH_2−YHCl absorptions sharpen on annealing the matrix samples to 28 K, but the CH_2−YHBr bands double in absorbance. This means that the Y + CH_3Br reaction to form CH_3−YBr is spontaneous and that the exothermicity is sufficient

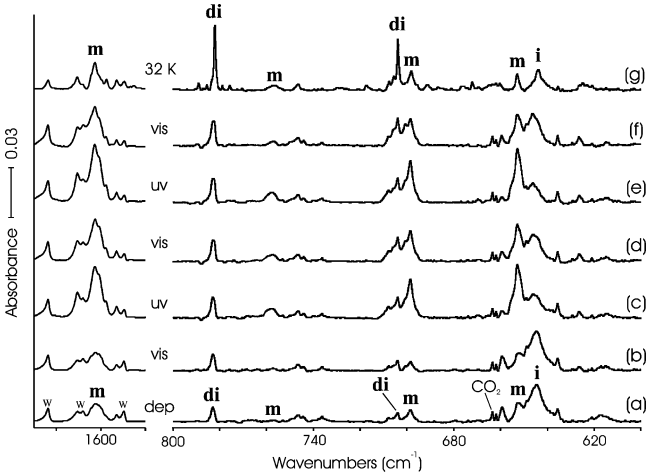

Figure 3. Infrared spectra for laser-ablated Ti and CH_3F reaction products in solid argon at 7 K: (a) for Ti and 0.2% CH_3F in argon codeposited for 1 h; (b) after visible irradiation (>530 nm); (c) after UV irradiation (240−380 nm); (d) after a second visible irradiation; (e) after a second UV irradiation; (f) after a third visible irradiation; (g) after annealing the sample to 32 K. W denotes water impurity absorptions.

to activate α-H transfer to form the CH_2−YHBr complex in the cold argon matrix.

$$Y + CH_3Br \rightarrow [CH_3{-}YBr]^* \rightarrow [CH_2{-}YHBr]^* \rightarrow CH_2{-}YHBr \quad (1)$$

The Y and CH_4 activation reaction follows suit. A 1409.7 cm^{-1} absorption increases on visible irradiation, whereas a 1421.6 and 1370.3 cm^{-1} band pair grows markedly on UV irradiation. Our calculations predict an almost C_{2v}-symmetric CH_2−YH_2 radical with a C−Y bond length of 2.322 Å and two very strong IR absorptions at 1469 and 1423 cm^{-1} and a C_s CH_3−YH radical with a C−Y length of 2.325 Å and one very strong IR band at 1454 cm^{-1}. The above pair of Y−H stretching modes is accordingly due to CH_2−YH_2 and the single 1409.7 cm^{-1} band to CH_3−YH. The fluorine substituent in this case appears to stablilize in a slight way the C−Y bond.[44]

Group 4

The goal of our matrix-isolation investigation was to characterize the titanium methylidene dihydride or "titanoethylene" molecule CH_2═TiH_2, but we knew from earlier methane activation experiments that the product yield would be relatively low. Hence, we reasoned that the analogous reactions with the more electron rich methyl halides would be more favorable, and the Ti and CH_3F reaction became our maiden voyage into the methylidene field.[30]

Figure 3 shows representative spectra of Ti and CH_3F reaction products. The initial sample deposit reveals three sets of IR absorptions that are grouped by their behavior on sample irradiation and annealing. The first set (labeled **m** for methylidene) at 1602.8, 757.9, 698.6, and 652.8 cm^{-1} decreases on visible light irradiation but increases markedly on UV irradiation, while the second set at 646.3 cm^{-1} (also 1105.7 and 504.3 cm^{-1}, not shown) (labeled **i** for insertion product) decreases. These photochemical cycles are reversible (Figure 3). Bands labeled **di** at 782.3 and 703.8 cm^{-1} (for dimethyltitanium difluoride) increase slightly on UV irradiation and markedly on annealing and with higher CH_3F reagent concentrations.

DFT calculations were performed using large Gaussian basis sets with extensive polarization functions, and the lowest energy

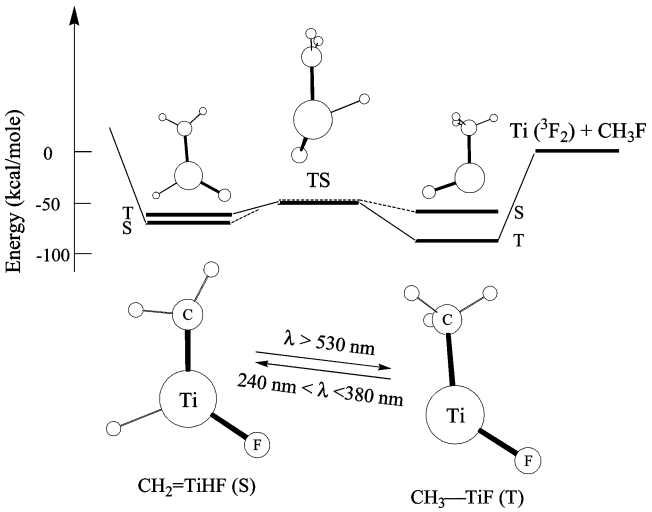

Figure 4. Reversible photochemical α-H transfer between CH_3—TiF and CH_2═TiHF. Triplet CH_3—TiF is converted to singlet CH_2═TiHF by UV irradiation on the triplet potential energy surface followed by intersystem crossing, which is reversed by visible irradiation on the singlet surface followed by intersystem crossing. The higher energy singlet CH_3—TiF, triplet transition state, and triplet CH_2—TiHF structures are shown above their calculated energy levels. S and T denote singlet and triplet spin states, and TS indicates the transition state.

products were CH_3—TiF (triplet state) and CH_2═TiHF (singlet state) with the latter 22 kcal/mol higher energy than the former. The observed frequencies for the **i** group correlated with the calculated frequencies having the higher IR intensities for CH_3—TiF, and the **m** group absorptions correspond with the strongest calculated IR frequencies for CH_2═TiHF. The detailed matching of shifts with $^{13}CH_3F$ and CD_3F and computed isotopic frequencies given in our original paper confirms the vibrational assignments and the molecular identity.[30a] Generally, B3LYP frequencies are a few percent above the observed values.[57,58] The 782.3 and 703.8 cm^{-1} flagship absorptions for the **di** group reveal Ti isotopic splittings in natural abundance for the antisymmetric and symmetric stretching vibrations of a TiF_2 subunit, and the associated 1385.2 and 1378.4 cm^{-1} bands are characteristic of methyl bending modes and the 566.9 cm^{-1} band (not shown) with the antisymmetric Ti—CH_3 stretching mode. The **di** bands are in excellent agreement with frequencies predicted for the $(CH_3)_2TiF_2$ molecule, which is analogous to the case for the $(CH_3)_2TiCl_2$ compound previously synthesized.[30b,60]

The persistent photoreversible nature of the **i** and **m** absorptions is noteworthy. α-Hydrogen transfer appears to be reversible on the triplet and singlet potential energy surfaces and to involve higher energy CH_2—TiHF (triplet) and CH_3—TiF (singlet) states in spin-allowed electronic transitions. With the global minimum energy CH_3—TiF (triplet) species as the starting point, UV absorption through a triplet transition state to the higher energy CH_2—TiHF (triplet) occurs followed by relaxation in the argon matrix to the CH_2═TiHF (singlet) state. In the reverse process, the CH_2═TiHF (singlet) state absorbs visible light through a singlet transition state to the higher energy CH_3—TiF (singlet) state, which is followed by matrix relaxation to the ground CH_3—TiF (triplet) state.[30a] The singlet methylidene is stable in the matrix, even though it is 22 kcal/mol higher in energy than the triplet insertion product: this stability arises from the singlet transition state energy barrier (18 kcal/mol) for reverse H transfer

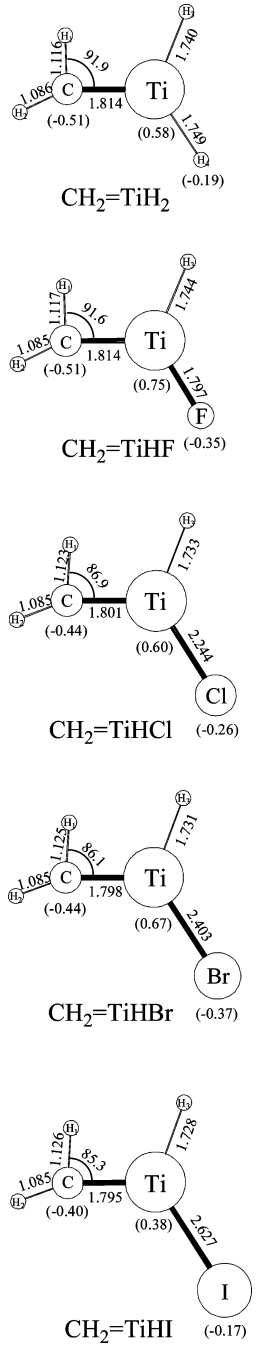

Figure 5. Structures calculated for CH_2═TiHX complexes at the B3LYP/6-311++G(2d,p) level of theory (SDD for I only). Bond lengths are in angstroms and angles in degrees. Mulliken charges are given for C, Ti, and X atoms.

in the ground singlet methylidene and shows the need for photoexcitation to drive the reversible α-H transfer process (Figure 4). This photoreversible α-H transfer process, summarized on the cover of this issue, led to the identification of these novel complexes.

The computed structure for CH_2═TiHF reveals a H′—C—Ti angle of 91.6° (H′ is the agostic hydrogen atom), and agostic distortion of the CH_2 subgroup, as illustrated by the structure in Figure 5. The trans-agostic structure is 4.2 kcal/mol more stable than the analogous cis-agostic form, on the basis of a fixed-point B3LYP calculation for the latter using the large basis set for C and H and SDD for Ti. Furthermore, the trans-agostic structure is 3.4 kcal/mol more stable than a nondistorted form with both C—H bond lengths fixed at the average value found

(60) (a) McGrady, G. S.; Downs, A. J.; Bednall, N. C.; McKean, D. C.; Thiel, W.; Jonas, V.; Frenking, G.; Scherer, W. *J. Phys. Chem. A* **1997**, *101*, 1951.

Table 1. Calculated Natural Electron Charges, Structural Parameters, and Observed Frequencies for Group 4 CH_2═MHX Methylidine Complexes[a]

	Ti			Zr			Hf		
	F	Cl	Br	F	Cl	Br	F	Cl	Br
q(C)	−0.83	−0.784	−0.777	−1.07	−1.00	−0.99	−1.17	−1.11	−1.09
q(H_1)[b]	0.18	0.18	0.18	0.18	0.18	0.18	0.19	0.19	0.19
q(H_2)[b]	0.20	0.20	0.20	0.20	0.20	0.20	0.20	0.20	0.20
q(H_3)	−0.49	−0.381	−0.376	−0.49	−0.44	−0.43	−0.49	−0.46	−0.45
q(M)	1.49	1.24	1.21	1.85	1.56	1.49	1.96	1.68	1.62
q(X)	−0.61	−0.46	−0.43	−0.67	−0.50	−0.46	−0.69	−0.51	−0.47
r(C═M)	1.811	1.797	1.794	1.964	1.950	1.948	1.977	1.962	1.959
r(C−H_1)	1.114	1.121	1.123	1.114	1.120	1.122	1.109	1.118	1.120
∠(H_1−C−M)	92.3	87.0	85.9	95.1	90.0	89.2	99.0	91.5	90.4
r(M−H)	1.732	1.722	1.721	1.886	1.875	1.873	1.875	1.869	1.868
ν(M−H)	1602.8	1618.4	1619.0	1537.8	1554.0	1556.6	1604.6	1607.8	1609.7
ν(C═M)	757.8	766.5	774.7	740.0	749.1	752.9	755.1	766.9	769.1

[a] B3LYP calculations with 6-311++G(3df,3pd) basis sets for C, H, F, Cl, and Br and SDD effective core potential and basis for Ti, Zr, and Hf. Bond lengths are given in angstroms, bond angles in degrees, and frequencies in cm^{-1}. [b] Unchanged ±0.002 within a particular metal.

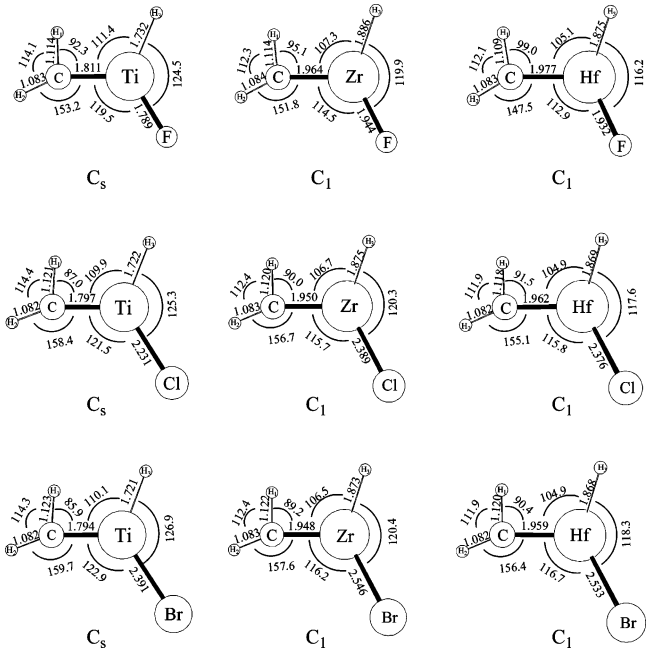

Figure 6. Structures calculated for group 4 CH_2═MHX methylidene complexes at the B3LYP/6-311++G(3df,3pd) level of theory (SDD for M only). Bond lengths are in angstroms and angles in degrees.

for the trans-agostic minimum. It appears that fluorine lone-pair repulsions may destabilize the cis-agostic form. In this regard, the CH_2═TiF_2 complex has been prepared recently, and B3LYP calculations reveal a symmetrical structure without agostic distortion, although the C═Ti bond is slightly longer, owing to the inductive effect of the extra fluorine substituent.[61]

Recently, Grunenberg et al. have used the CH_2═TiHF complex as a model to explore the agostic bond. These workers employed different theoretical methods and found virtually the same structure with the B3LYP density functional as in Figure 5 and a slightly stronger agostic interaction using the more rigorous CCSD(T) level of theory.[19]

The Zr and CH_3F reaction also gave the insertion product (CH_3−ZrF) and the methylidene complex (CH_2═ZrHF), but the latter bands were split into two photoreversible sets.[32] Different matrix packing configurations or "sites" often cause such splittings,[62] but it is unusual for the splittings to be as large or to be photoreversible. Hafnium and methyl fluoride combined[34] to give the methylidene CH_2═HfHF, and the computed structures for the Ti, Zr, and Hf species are compared in Figure 6. Notice that the agostic distortion decreases with increasing metal size in group 4 for all three halide species.

Just as methyl fluoride was more reactive with Ti than methane, methyl chloride and bromide produced even greater product yields, and the corresponding **i** and **m** absorptions were again photoreversible with visible and UV light.[36] Several frequency trends are noteworthy, and these are summarized in Table 1. The computed agostic H′−C−Ti angle decreases, the C═Ti bond length decreases, and the Ti−H bond length decreases with increasing halogen size (Figure 5), which are in accord with the observed increases in the C═Ti and Ti−H stretching frequencies. Clearly the agostic interaction increases with increasing halogen size. This is accompanied by a charge flow from carbon, hydride (H_3), and halide to the metal center, while the hydrogens on carbon are unchanged, which is in general accord with the approximate model of computed Mulliken charges (Figure 5).

To test these trends, similar experiments were performed with CH_3I and CD_3I, and analogous new absorptions were observed for CH_3−TiI (1110.8, 512.0 cm^{-1}), CD_3−TiI (866.8, 453.2 cm^{-1}), CH_2═TiHI (1619.8, 772.0, 647.8, and 626.8 cm^{-1}), CH_2═TiDI (1169.4, 513.8 cm^{-1}), $(CH_3)_2TiI_2$ (1366.3, 539.8 cm^{-1}), and $(CD_3)_2TiI_2$ (1003.7, 916.8, 489.1 cm^{-1}), which will be reported here. Assignment is based on comparison with the methyl chloride and bromide observations and calculated frequencies (Table S1 in the Supporting Information compares observed and calculated frequencies for the methylidene species).

The trend of increasing agostic interaction F < Cl < Br continues with I, as shown by the calculated structures in Figure 5. In contrast to the lighter methyl halide reactions, CH_3I reacts with Ti atoms on annealing the argon matrix to produce a 3-fold increase in the CH_2═TiHI absorptions. This means that the insertion reaction and the following α-H transfer are spontaneous in this system, as described above for Y and methyl bromide.

The dimethyltitanium dihalide molecules were observed for all four methyl halides, which shows that a second methyl halide molecule is activated by CH_3−TiX and/or CH_2═TiHX. This is particularly significant in the case of $(CH_3)_2TiCl_2$, as this compound has been investigated separately, and our absorptions are in agreement.[60]

Similar experiments with Zr, Hf, CH_3Cl, and CH_3Br give IR absorptions for the analogous CH_3−MX and CH_2═MHX complexes.[43] Diagnostic frequencies in the series are included in Table 1. A similar relationship of increasing agostic interaction with increasing halogen size is found in calculated structures

(61) Lyon, J. T.; Andrews, L. *Organometallics* **2006**, *25*, 1341.
(62) Jacox, M. E. *Chem. Phys.* **1994**, 189, 149.

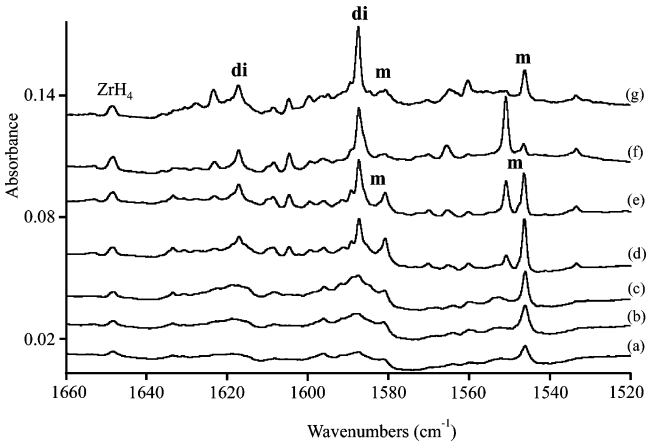

Figure 7. Infrared spectra in the Zr−H stretching region for laser-ablated zirconium and methane reaction products in solid neon at 5 K: (a) for Zr codeposited with 0.4% CH_4 in neon for 45 min; (b) after visible irradiation (>530 nm); (c) after UV irradiation (240−380 nm); (d) after annealing to 10 K; (e) after annealing to 11 K; (f) after annealing to 12 K; (g) after full UV irradiation (>220 nm).

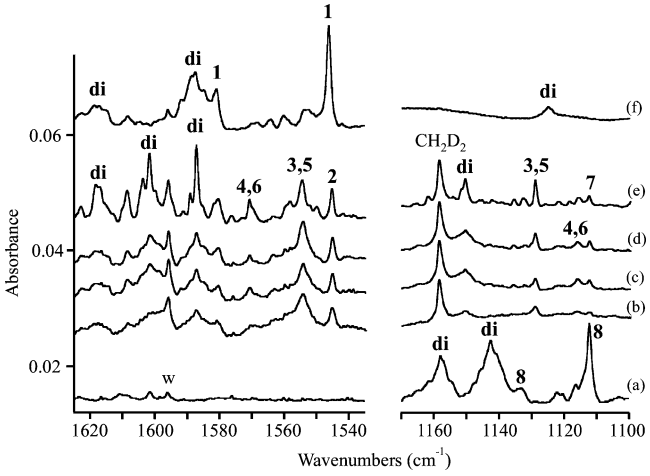

Figure 8. Infrared spectra in the Zr−H and Zr-D stretching regions for zirconium and isotopic methane reaction products in solid neon at 5 K: (a) for 0.4% CD_4, after visible and UV irradiation; (b) for 0.6% CH_2D_2; (c) after UV irradiation; (d) after visible irradiation; (e) after annealing to 11 K; (f) for 0.4% CH_4, after visible and UV irradiation.

(Figure 6) and observed frequencies (Table 1). The structures and natural electronic charges[63] were computed for the group 4 CH_2═MHX complexes to analyze the charge flow associated with the increasing agostic interaction as a function of halide for each metal in these simple complexes. In this halogen series, the most electron-deficient metal center (highest positive charge) supports the weakest agostic interaction (longest C═M bond). The apparent inductive effect sustains an increase in the agostic interaction (shortest C═M bond) with the larger halogen. Finally, the methylidene bands were split into photoreversible pairs, which have been attributed to the argon or krypton matrix trapping the less stable planar and the more stable pyramidal forms of the methylidene complexes.

The simple CH_2═ZrH_2 complex presents the best experimental case for agostic distortion in a methylidene dihydride complex.[18,33] Figure 7 illustrates the neon matrix spectrum for laser-ablated Zr codeposited with 2% CH_4 in neon at 4 K. Weak bands were observed near 1581.0 and 1546.2 cm^{-1} (labeled **m**) on sample deposition. These absorptions exhibit splittings (broad 1586 and sharp 1551.0 cm^{-1} absorptions) due to matrix trapping of slightly different ZrH_2 out-of-plane configurations that are reversed on UV irradiation and annealing. The **m** bands increase on visible and UV irradiation and sharpen on annealing, and annealing also substantially increases absorptions at 1617.2 and 1587.6 cm^{-1} (labeled **di**). The **di** bands are favored markedly relative to the **m** absorptions at higher CH_4 concentrations. The aforementioned absorptions in the Zr−H stretching region have counterparts in the Zr−D stretching region (Figure 8a) and the H/D frequency ratios, 1.3953 and 1.3901, characterize these vibrations as symmetric and antisymmetric Zr−H_2 stretching modes. Note that these new Zr−H_2 stretching modes appear between the 1530 and 1648 cm^{-1} antisymmetric stretching modes for ZrH_2 and ZrH_4 in solid neon.[18] Two absorptions at 757.0 and 634.5 cm^{-1}, which show carbon-13 shifts appropriate for C═Zr stretching and CH_2 wagging modes, are associated with species **m**, and four absorptions at 1375.1, 1125.0 cm^{-1} in the methyl deformation region and at 593.4, 564.2 cm^{-1} track with the **di** bands.

Chart 1

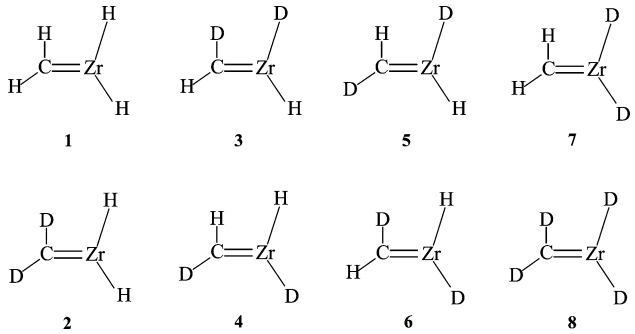

The CH_2D_2 reaction provides diagnostic information for the identification of the **di** and **m** species. Figure 8 shows a single mixed H/D intermediate component between two Zr−H and two Zr−D **di** absorptions, which characterizes the stretching vibrations of two equvalent Zr−H bonds. In contrast, the appearance of two intermediate bands for species **m** (labeled **3,5** and **4,6**) in each region characterizes the stretching vibration of two structurally nonequivalent Zr−H bonds. This evidence is critical for the experimental documentation of agostic distortion; therefore, the isotopic shifts will be reviewed here. If there were no agostic distortion, the two possible products would be *cis*- and *trans*-CHD═ZrHD, and these two isotopomers have the same computed Zr−H and Zr−D stretching modes (±0.1 cm^{-1}).[18] Hence, one new mixed isotopic band would be observed for the symmetrical methylidene, but in contrast, we have observed two mixed isotopic bands which document that the methylidene product is distorted to produce two nonequivalent Zr−H bonds.

The eight isotopic molecules are sketched in Chart 1 (labeled **1** for all H and **8** for all D). Our isotopic frequency calculations predict that **3** and **5** have the same Zr−H and Zr−D stretching modes (±0.2 cm^{-1}) blue-shifted 8 and 18 cm^{-1} from **2** and **7**, and **4** and **6** have the same such modes blue-shifted 23 and 4 cm^{-1}. The bands labeled **3,5** and **4,6** are 8 and 17 cm^{-1} and 25 and 4 cm^{-1} blue-shifted. This excellent agreement between computed and observed CHD═ZrHD isotopic shifts for the Zr−H and Zr−D stretching chromophore confirms the distortion of CH_2═ZrH_2 in the inert neon matrix.

The final confirmation for the identification of CH_2═ZrH_2 is the agreement between calculated and observed frequencies

(63) Reed, A. E.; Curtiss, L. A.; Weinhold, F. *Chem. Rev.* **1988**, *88*, 899.

Table 2. Vibrational Frequencies Observed and Calculated for the C_1 Ground-State Structure of $CH_2{=}ZrH_2$ at the CCSD/6-311++G(2d,p)/SDD and B3LYP/ 6-311++G(3df,3pd)/SDD Levels of Theory

mode	calcd[a]	intens[b]	calcd[c]	intens[b]	obsd[d]	ratio[e]
CH_2 str	3210	1	3179	1		
CH_2 str	2842	7	2858	5		
ZrH_2 str	1650	384	1634	301	1581	0.968
ZrH_2 str	1597	695	1603	544	1546	0.964
CH_2 scis	1384	17	1320	16		
C=Zr str	787	133	767	130	757	0.987
CH_2 wag	713	206	665	144	635	0.955
ZrH_2 scis	656	55	642	85		
ZrH_2 rock	531	29	515	10		
CH_2 twist	481	3	408	23		
CH_2 rock	385	6	310	75		
ZrH_2 wag	87	457	240	131		

[a] CCSD, in cm^{-1}. [b] Intensities in km/mol. [c] B3LYP, in cm^{-1}. [d] Neon matrix. [e] Ratio obsd/B3LYP calcd (i.e., scale factor).

for four diagnostic modes. Table 2 gives the frequencies calculated (not scaled) for the C_1-symmetric $CH_2{=}ZrH_2$ structure at the B3LYP and CCSD levels of theory.[18,64] Note that the four most intense calculated frequencies are 3.2, 3.6, 1.3, and 4.5% higher, as is appropriate for this density functional,[57,58] and the more rigorous quantum-mechanical CCSD method gives slightly higher frequencies, which correlate well with the experimental absorptions. (The calculated and observed $^{13}CH_2{=}ZrH_2$ and $CD_2{=}ZrD_2$ frequencies are discussed in the original report.[18]) Thus, we conclude that $CH_2{=}ZrH_2$ is distorted by agostic interaction, on the basis of our neon (and argon) matrix spectra and calculations at several levels of single reference theory. The small T1 diagnostic that we obtained (0.016) indicates that multireference character is not a problem for $CH_2{=}ZrH_2$.[64,65] Although multireference calculations found a stable C_{2v} structure after imposing C_{2v} symmetry,[13] we believe that the lowest energy structure is distorted, as we have described here.

The six **di** frequencies identify the $(CH_3)_2ZrH_2$ molecule with C_{2v} skeletal symmetry. This is the first observation of a group 4 metal dimethyl dihydride.[18] The $(CH_3)_2TiH_2$ and $(CH_3)HfH_2$ analogues have also been characterized.[31,35] The more stable Cp_2MH_2 compounds are known organometallic reagents.[66] Previous work involving photoexcitation of Ti in pure methane "failed to yield insertion products."[25] Our experiments with Ti and 1% CH_4 in argon produced $CH_3{-}TiH$ and $CH_2{=}TiH_2$ on UV irradiation along with a small yield of $(CH_3)_2TiH_2$. The latter increased markedly on annealing, which shows that the primary reaction products activate a second CH_4 molecule.[31] The pure methane experiments failed either because the appropriate range of photoexcitation wavelengths was not employed or because the initial product reacted further in the pure methane environment.

Analogous CH_4 reactions with Ti and Hf give methylidene products as well.[31,35] The B3LYP(DFT) structures compared in Figure 9 show again that the agostic distortion decreases on going from Ti to Zr to Hf. Calculations were also performed with the CCSD method and 6-311++G(2d,p) basis (SDD for Zr,Hf), and similar distorted structures were obtained (H′−C−M angles are 89.6, 90.1, and 90.4°, and C=M distances are 1.852, 1.964, and 1.972 Å). Furthermore, Grunenberg has calculated

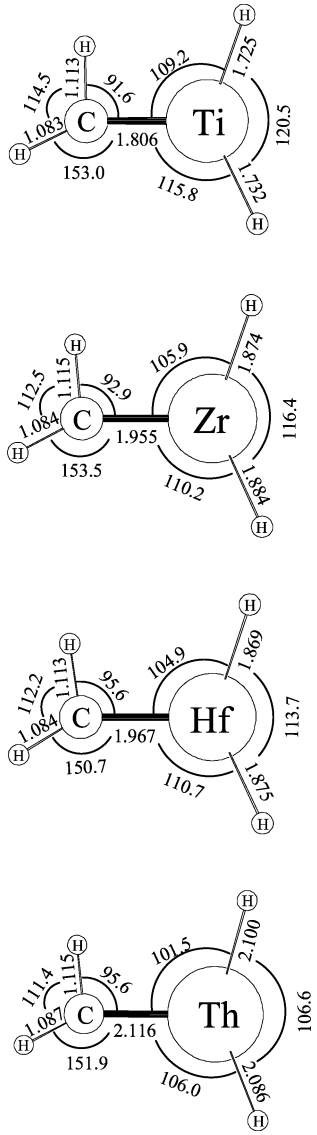

Figure 9. Structures calculated for $CH_2{=}MH_2$ methylidene dihydride complexes (M = Ti, Zr, Hf, Th) at the B3LYP/ 6-311++G(3df,3pd) level of theory (SDD for M only). Bond lengths are in angstroms and angles in degrees.

$CH_2{=}TiH_2$ at the more rigorous CCSD(T) level of theory, found an even stronger agostic interaction (the agostic angle is 84.6 or 83.5° and C=Ti bond length is 1.848 or 1.840 Å, depending on the basis set) (Figure 10), and has pointed out that the dynamic correlation employed in DFT and CCSD(T) may be more important than multireference character for determining the structure of $CH_2{=}TiH_2$.[67]

The agostic bonding phenomenon was first described by Brookhart and Green to characterize the attraction of C−H bonding electrons for an electron-deficient metal center and the resulting structural distortion.[6] Such interactions have been identified many times in the ensuing decades and described more generally in two excellent recent review articles. In particular, Clot and Eisenstein and Scherer and McGrady have reported that agostic stabilization has little or no dependence on C−H→M electron donation but arises from delocalization of the C=M bonding electrons.[9,10]

What can we learn about the agostic interaction from computations on the simple zirconium methylidene dihydride

(64) Cho, H.-G.; Andrews, L. New calculations done for this review article, 2006.

(65) Lee, T. J.; Taylor, P. R. *Int. J. Quantum Chem. Symp.* **1989**, *23*, 199.

(66) (a) Roddick, D. M.; Fryzuk, M. D.; Seidler, P. F.; Hillhouse, G. L.; Bercaw, J. E.. *Organometallics* **1985**, *4*, 97. (b) Chen, E. Y.-X.; Marks, T. J. *Chem. Rev.* **2000**, *100*, 1391.

(67) Grunenberg, J. Personal communication of unpublished work, 2006.

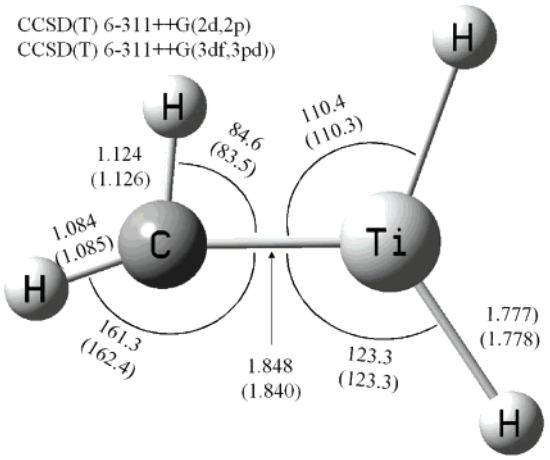

Figure 10. Structure and bond lengths and angles calculated for $CH_2{=}TiH_2$ methylidene dihydride at the CCSD(T) level of theory using two all-electron basis sets. Bond lengths are in angstroms and angles in degrees for planar molecule. Top data are from the 6-311++G(2d,2p) basis set and bottom data in parentheses are from the 6-311++G(3df,3pd) basis set calculation. (Figure courtesy of J. Grunenberg.)

Table 3. Comparison of Parameters Calculated by Different Theoretical Methods for the Description of Agostic Bonding in $CH_2{=}ZrH_2$

method	H′−C−Zr	H′−C	C=Zr	Zr−H	H′- - -Zr
B3LYP[b]	95.5	1.114	1.961	1.882	2.345
B3LYP[c]	92.9	1.115	1.955	1.884	2.300
CCSD[b]	90.1	1.123	1.964	1.895	2.264
CCSD[c]	86.1	1.124	1.942	1.888	2.176
BPW91[c]	85.5	1.135	1.943	1.879	2.172
CCSD(T)[c]	83.8	1.130	1.947	1.884	2.144
MP2[c]	80.1	1.133	1.927	1.867	2.061

[a] The agostic hydrogen is H′, and the given Zr−H is trans to H′. Bond lengths are given in angstroms and bond angles in degrees. [b] 6-311++G(2d,p)/SDD basis sets. [c] 6-311++G(3df,3pd)/SDD basis sets.

subject complex? We have shown that polarization functions are necessary to describe the agostic distortion.[18] Different theoretical methods offer different descriptions of the covalent and electrostatic contributions to this bonding interaction, and Table 3 compares the results of two density functional and two ab initio methods and two basis sets. The MP2 method overestimates the effect, the B3LYP density functional underestimates the bonding, and the more rigorous CCSD(T) method gives an intermediate result. These C=Zr bond lengths are slightly shorter than the 2.024 Å value measured for a representative ligand-stabilized zirconium alkylidene complex.[68] It is clear that basis sets with more polarization functions support a stronger agostic interaction.

Let us consider symmetrical $CH_2{=}ZrH_2$ with two symmetry planes (C_{2v}) and then relax to one horizontal plane of symmetry (C_s) and finally to no symmetry (C_1). Figure 11 shows these three structures calculated at the CCSD(T) level of theory.[56,64] First, the C_{2v}-symmetric $CH_2{=}ZrH_2$ complex has two imaginary frequencies (CH_2 rock and ZrH_2 wag) and has 3.0 kcal/mol higher energy than the C_1 minimum, and the C_s molecule has one imaginary frequency (ZrH_2 wag) and has 0.5 kcal/mol higher energy than the C_1 minimum, which has all real frequencies. Second, notice that the C=Zr and average ZrH_2 bond lengths decrease and the "agostic" C−H bond length increases while the other C−H bond length decreases as the

(68) Fryzuk, M. D.; Mao, S. S. H.; Zaworotko, M. J.; MacGillivray, L. R. *J. Am. Chem. Soc.* **1993**, *115*, 5336. (C−Zr bond).

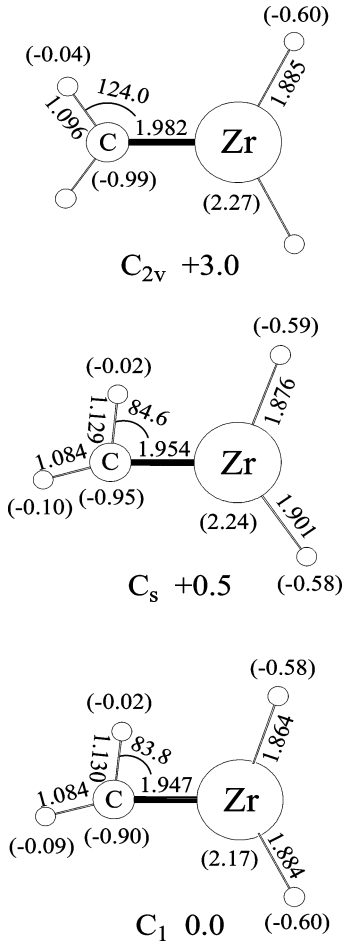

Figure 11. Structures calculated for $CH_2{=}ZrH_2$ at the CCSD(T)/6-311++G(3df,3pd)/SDD (for Zr) level of theory to illustrate the agostic distortion process: (top) C_{2v} symmetry imposed; (middle) fixed horizontal plane of symmetry (C_s), (bottom) no symmetry (C_1) minimum energy structure. Bond lengths (angstroms), bond angles (degrees), Mulliken charges, and relative energies (kcal/mol) are given for each structure.

energy is lowered. Third, the Mulliken charges calculated for C and Zr atoms are given in the structures. What is important here is not the absolute values of the charges but the changes that accompany structural relaxation. The major change is charge flow from negative carbon to positive zirconium, reducing the bond polarity. Notice that the (longer bond) agostic H on carbon becomes less negative and the (shorter bond) other H on carbon becomes more negative, and the total negative charge on the CH_2 group decreases on structural relaxation. The same relationship is found for both Mulliken and natural charges computed at the B3LYP level.

The changes described above (Figure 11) show that agostic bonding involves the electronic reorganization, structural relaxation, and energy lowering for the entire methylidene complex. Hence, agostic bonding is identified by CH_2 distortion, but the C=M bond and its ligands are intimately involved as well. These changes are clearly quantified and characterized here for the simple $CH_2{=}ZrH_2$ model methylidene system.

The $HN{=}TiH_2$ complex is isoelectronic with $CH_2{=}TiH_2$, whose structure clearly shows the effect of agostic distortion (Figure 10). How will agostic interaction be manifested in the $HN{=}TiH_2$ species, which has a lone electron pair and a N−H bond pair on the nitrogen to compete for interaction with the titanium center? Zhou et al. have prepared the novel $HNTiH_2$ molecule and computed a $^1A'$ ground-state structure with a short

Ti═N bond (1.663 Å) and slightly bent Ti═N−H angle (170.6°), all in the plane bisecting the TiH_2 angle.[69] The lone pair is clearly interacting more strongly with the metal center than the N−H bond, which is different from the typical $HN{=}CR_2$ organic imine structure. Hence, agostic distortion in the $HN{=}TiH_2$ case moves the N−H bond *away* so that the lone pair can interact more favorably with the titanium center to stabilize and even increase the N═Ti double bond.

Group 5

Niobium reactions were performed with CH_3F, and three groups of new absorptions were observed and characterized by their photolysis behavior.[41] A weak band at 629.7 cm^{-1} destroyed by visible light was assigned to the insertion product CH_3−NbF. The second set of five bands led by a strong 1698.7 cm^{-1} Nb−H stretching absorption increased on visible and UV irradiation and characterized the methylidene species $CH_2{=}NbHF$. The third group of six bands followed two Nb−H stretching absorptions at 1560 and 1526.7 cm^{-1} by increasing on visible and decreasing on UV irradiation and by elimination on doping with CCl_4. The halocarbon preferentially captures ablated electrons and prevents the formation of molecular anions.[50] Accordingly, calculations were done for the stable $CH{\equiv}NbH_2F^-$ anion, and agreement between calculated and observed isotopic frequencies substantiated this identification of the first group 5 methylidyne anion complex.[41] Tantalum alkylidyne complexes have been prepared using stabilizing trimethphosphine ligands,[70] but we have found no previous experimental evidence for a niobium alkylidyne complex or a group 5 methylidyne anion complex.

The $CH_2{=}NbHF$ complex reveals slightly more agostic distortion than $CH_2{=}ZrHF$, as shown by the calculated structures in Figure 2. To examine substituent effects, the analogous CH_3Cl and CH_3Br reactions were explored to find similar major products.[71] The methylidene complexes $CH_2{=}NbHCl$ and $CH_2{=}NbHBr$ are characterized by strong Nb−H stretching modes at 1697.9 and 1698.9 cm^{-1}, respectively, and calculated structures that show small changes from that for $CH_2{=}NbHF$. For the Cl and Br derivatives, the agostic H′−C−Nb angles decrease to 88.9 and 87.9°, the C═Nb bond lengths decrease to 1.881 and 1.878 Å, and the Nb−H lengths decrease to 1.797 and 1.794 Å, respectively. It appears that the agostic interaction in $CH_2{=}NbHX$ complexes increases with halogen size, just as with group 4, but the effect is slightly less for the Nb methylidyne complexes.

Vanadium and methyl fluoride produce both CH_3−VF and $CH_2{=}VHF$, which are photoreversible, like the Ti analogues discussed earlier, and show a kinetic isotope effect on the yield of $CD_2{=}VDF$.[71] The Ta and CH_3Cl reaction forms $CH_2{=}TaHCl$ straightaway, and this product increases dramatically on sample annealing. Thus, atomic Ta spontaneously activates CH_3Cl through rearrangement of CH_3−TaCl directly to the more stable methylidene complex.[71]

The codeposition of laser-ablated Nb atoms with 2% methane diluted in argon produced new IR absorptions at 1680.7 and 1652.5 cm^{-1} (labeled **m**), at 1611.4 cm^{-1} (labeled **i**), and at 1542.5 and 1489.5 cm^{-1} (labeled **a**), as shown in Figure 12b.[42] Irradiation in the visible region increased the **m** bands threefold with little effect on the other bands, whereas ultraviolet light slightly decreased the **a** bands, increased the **m** bands, and produced weak new 1717.5 and 1686.3 cm^{-1} bands (labeled **di**). Subsequent annealing to 26 K increased the **di** bands slightly at the expense of the **m** bands. Similar experiments with CD_4 gave appropriately shifted spectra, as shown in the lower half of Figure 12, and the growth of **m** bands on visible irradiation was even more pronounced. In addition, only the **a** bands were eliminated on the addition of CCl_4 to the sample[14] (Figure 12a).

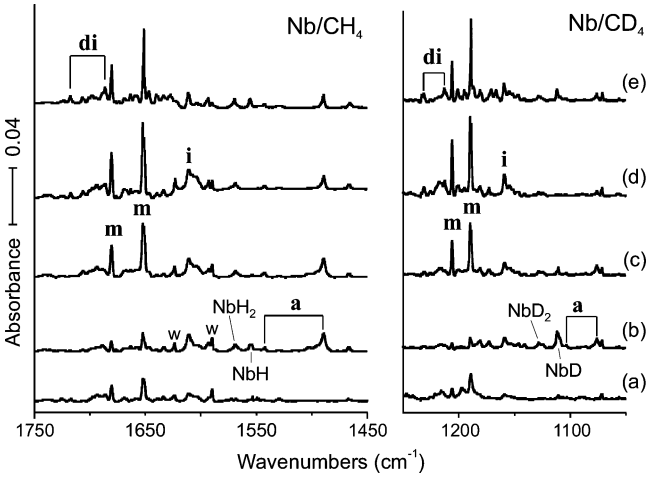

Figure 12. Infrared spectra in the regions of 1750−1450 and 1250−1050 cm^{-1} for laser-ablated Nb atoms codeposited with CH_4 and CD_4, respectively, in excess argon at 8 K: (a) after codeposition of Nb + [2% methane + 0.04% CCl_4] in Ar for 1 h and visible irradiation (>420 nm); (b) Nb + 2% methane in Ar codeposited for 1 h; (c) after visible irradiation; (d) after full UV irradiation (λ > 220 nm); (e) after annealing to 26 K. The m, i, a, and di labels indicate new product absorption groups.

The two major product absorptions at 1680.7 and 1652.5 cm^{-1} show large deuterium shifts (H/D isotopic ratios 1.394 and 1.389) and no carbon-13 displacement. The appearance of these bands just above known NbH_2 absorptions at 1610.4 and 1569.0 cm^{-1} suggests assignment to the $CH_2{=}NbH_2$ methylidene. The observation of an associated band at 805.4 cm^{-1} with a large carbon-13 shift, which is appropriate for a C═Nb stretching mode, and bands at 547.1 and 480.4 cm^{-1} with small and zero carbon-13 shifts, which are expected for lower frequency CH_2 and NbH_2 motions, substantiates this assignment. Tantalum forms the analogous methylidene complex, but the vanadium species is too high in energy to be produced in these experiments.[42]

The CH_2D_2 reaction products provide diagnostic information regarding the structure of $CH_2{=}NbH_2$. Triplet **m** absorptions with strong, sharp new median bands at 1608.7, 1666.4, 1652.5 cm^{-1} and at 1205.5, 1198.4, 1188.7 cm^{-1} show that the two Nb−H bonds are equivalent. The 1680.7 and 1652.5 cm^{-1} bands are then due to $CH_2{=}NbD_2$, the 1205.5 and 1188.7 cm^{-1} bands to $CD_2{=}NbH_2$, and the strong median 1666.4 and 1198.4 cm^{-1} bands to CHD═NbHD. The $CH_2{=}ZrH_2$ complex exhibited an agostic interaction, which resulted in distortion at CH_2 and ZrH_2 such that the two Zr−H bonds were not equivalent, which was manifested in the experimental spectrum and calculated frequencies for the CHD═ZrHD and CDH═ZrDH isotopic molecules. In contrast, niobium forms only one CHD═NbHD isotopic molecule, as the two Nb−H bonds are equivalent.

The single **i** absorption at 1611.4 cm^{-1} just below the **m** bands shows little change on photolysis, in contrast to the **m** bands. The band shifts to 1159.1 cm^{-1} with CD_4 (H/D ratio 1.390) and is unchanged with $^{13}CH_4$. In the reaction of transition-metal atoms with methane, the monohydride insertion product is formed first, and this M−H absorption is just lower than the

(69) Chen, M.; Lu, H.; Dong, J.; Miao, L.; Zhou, M. *J. Phys. Chem. A* **2002**, *106*, 11456.

(70) McLain, S. J.; Wood, C. D.; Messerle, L. W.; Schrock, R. R.; Hollander, F. J.; Youngs, W. J.; Churchill, M. R. *J. Am. Chem. Soc.* **1978**, *100*, 5962.

(71) Cho, H.-G.; Andrews, L. *J. Phys. Chem. A*, in press (group 5 + CH_3X).

$CH_2{=}MH_2$ product. Our calculations predict a quartet state $CH_3{-}NbH$ product with one strong Nb−H stretching frequency about 40 cm^{-1} below the strongest absorption of $CH_2{=}NbH_2$. The 1611.4 cm^{-1} band is therefore assigned to the $CH_3{-}NbH$ insertion product, which can undergo α-H transfer to form the methylidene complex.[42]

The **a** absorptions at 1542.5 and 1489.5 cm^{-1} are the lowest product absorptions in the Nb−H stretching region, even lower than those of the binary hydride products NbH_2 and NbH, which are observed here as weak bands at 1569.1 and 1555.9 cm^{-1}. The **a** bands show no carbon-13 shift and deuterium counterparts at 1103.7 and 1076.1 cm^{-1} (H/D ratios 1.398 and 1.384), which are appropriate for symmetric and antisymmetric Nb−H stretching modes. The **a** absorptions are stable to visible irradiation, but they decrease slightly with 220 nm irradiation. The most important diagnostic is the absence of the **a** bands in the presence of CCl_4 (Figure 1a), which captures ablated electrons, suggesting that the **a** bands are due to a molecular anion.[50] Our calculations predict a very strong antisymmetric Nb−H stretching absorption for singlet $CH{\equiv}NbH_3^-$ in a C_{3v} structure at 1540 cm^{-1}, which is 190 cm^{-1} below the strongest band for $CH_2{=}NbH_2$, and the 1489.5 cm^{-1} band is 163 cm^{-1} below the **m** absorption. A symmetric Nb−H absorption 25% as strong is also predicted 43 cm^{-1} higher, and the associated 1542.5 cm^{-1} band is in agreement. Thus, the **a** bands can be assigned with confidence to the symmetric and antisymmetric Nb−H stretching modes for $CH{\equiv}NbH_3^-$, the simple niobium trihydride methylidyne anion. This anion is 42 kcal/mol more stable than $CH_2{=}NbH_2$ and an extra electron, which suggests that electron capture fosters another α-H transfer to give the stable methylidyne anion. The analogous $CH{\equiv}NbH_2F^-$ anion complex has slightly higher frequencies at 1560 and 1527 cm^{-1}. Finally, tantalum forms similar methylidyne anion complexes.[42,71]

The two **di** bands at 1717.5 and 1686.3 cm^{-1} track together and shift to 1231.5 and 1213.0 cm^{-1} on deuterium substitution (H/D ratios 1.395 and 1.390), which suggests symmetric and antisymmetric stretching modes of another $X{-}NbH_2$ species. These bands increase on full arc photolysis, particularly with higher methane concentration, which indicates a higher order product in methane. Our calculations predict the $(CH_3)_2NbH_2$ dihydride to be 28 kcal/mol more stable than $CH_2{=}NbH_2$ and CH_4 together and to have Nb−H stretching frequencies 3 and 28 cm^{-1} above the higher band of the methylidene, in line with the higher oxidation state of the metal center, which fits the observed spectrum very well. The activation of a second methane molecule by $CH_2{=}ZrH_2$ was spontaneous on annealing the matrix to allow diffusion and reaction, but full-arc irradiation was required to initiate this reaction in the niobium system.

Group 6

Our motivation for investigating group 6 reactions with CH_3F was to explore the possibility that further α-H transfer in the analogous methylidene complex might form a methylidyne complex. Indeed, two distinctly different sets of photoreversible product bands were observed for Mo and W reactions, and the photoreversibility was particularly impressive for Mo.[37] Infrared spectra for this system are illustrated in Figure 13. The most intense I band at 589.3 cm^{-1} was assigned to the Mo−F stretching mode of the primary insertion product $CH_3{-}MoF$, the most intense II band at 1797.7 cm^{-1} to the Mo−H stretching mode of $CH_2{=}MoHF$, and the most intense III band at 1844.8 cm^{-1} to the antisymmetric $Mo{-}H_2$ stretching mode of $CH{\equiv}MoH_2F$. Notice that visible photolysis decreases I and II and increases III, whereas UV irradiation reverses these changes, and these reversible cycles are repeated two times. These assignments and those of associated absorptions are substantiated by comparison with calculated frequencies.[37] The computed structures show a decrease in C−Mo bond length from 2.113 to 1.836 to 1.719 Å, respectively (see Figure 2 for $CH_2{=}MoHF$). The analogous tungsten products reveal computed C−W bond lengths from 2.112 to 1.898 to 1.748 Å. The experimental and computational evidence clearly supports the formation of these simple methylidyne complexes.[61] Finally, notice that agostic distortion increases in the $CH_2{=}MHF$ series (M = Y, Zr, Nb, Mo), as summarized in Table 4.

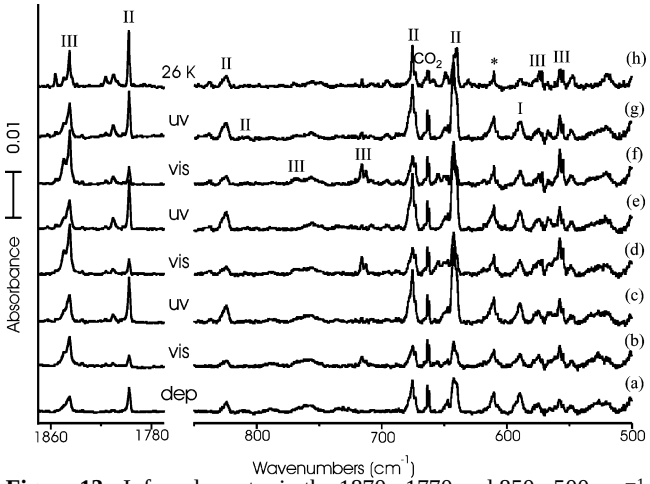

Figure 13. Infrared spectra in the 1870−1770 and 850−500 cm^{-1} regions for products of Mo atom reactions with methyl fluoride in solid argon at 7 K: (a) for Mo and 0.5% CH_3F in argon codeposited for 1 h; (b) after visible irradiation (>420 nm); (c) after UV irradiation (240−380 nm); (d) after visible irradiation; (e) after UV irradiation; (f) after visible irradiation; (g) after UV irradiation; (h) after annealing to 26 K.

Table 4. Mulliken Charges and Structural Parameters Calculated for the $CH_2{=}MHF$ Methylidenes (M = Y, Zr, Nb, Mo)[a]

	$CH_2{-}YHF$	$CH_2{=}ZrHF$	$CH_2{=}NbHF$	$CH_2{=}MoHF$
q(C)	−0.75	−0.84	−0.78	−0.74
$q(H_1)$	0.070	0.16	0.02	0.03
$q(H_2)$	0.049	0.14	0.00	0.01
q(M)	1.66	1.33	1.80	1.68
$q(H_3)$	−0.45	−0.20	−0.43	−0.33
q(F)	−0.57	−0.59	−0.61	−0.66
C=M (Å)	2.331	1.966	1.891	1.838
$H_1{-}C{-}M$ (deg)	124.1	95.1	92.4	84.5

[a] B3LYP/6-311++G(3df,3dp)/SDD.

Scheme 1

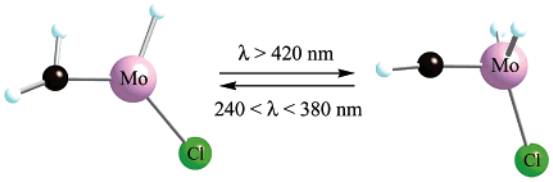

Analogous experiments have also been done for Mo, CH_3Cl, and CH_3Br, and we find the strong diagnostic II and III bands at 1789.5 and 1835.8 cm^{-1} for CH_3Cl and at 1787.3 and 1831.2 cm^{-1} for CH_3Br reaction products. These bands exhibit 1.391 and 1.396 H/D isotopic frequency ratios, as expected for a Mo−H stretching vibration. These halogen-substituted methylidene and methylidyne complexes also undergo reversible photochemical α-hydrogen transfer rearrangement,[72] as illustrated in Scheme 1. Another interesting observation is that

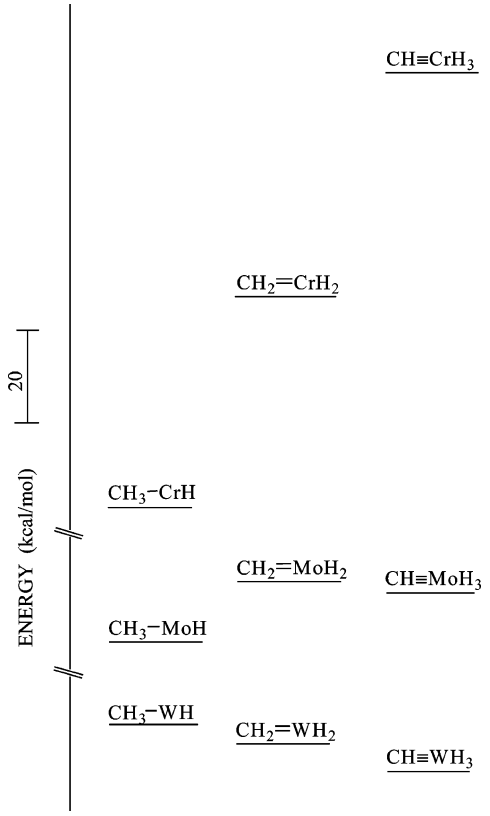

Figure 14. Relative energies calculated at the B3LYP/6-311++G(3df,3pd)/SDD level for the lowest electronic states of the CH_3−MH, CH_2=MH_2, and CH≡MH_3 molecules from group 6. The close-lying states of the Mo and W complexes are involved in reversible α-H transfer photochemistry.

the Mo−H stretching frequencies in CH_2=MoHX complexes decrease slightly, whereas the Zr−H stretching frequencies in CH_2=ZrHX complexes increase with increasing halogen size, as discussed above for group 4.

The analogous reactions with Cr gave only CH_3−CrF, but W produced CH_3−WF, CH_2=WHF, and CH≡WH_2F. The chromium methylidene and methylidyne complexes are apparently too high in energy to be formed here. Calculations performed at the more rigorous and more time-consuming CCSD level gave slightly higher frequencies with slightly different mode mixing based on isotopic shifts but essentially the same structures for CH_2=MoHF and CH_2=WHF complexes as the B3LYP density functional.[39]

Methane activation with group 6 atoms produces up to three products, and the relative energies provide a guide to the product yields.[40] Figure 14 displays the energies calculated for potential Cr, Mo, and W methylmetal hydride, methylidene, and methylidyne reaction products. Infrared spectra for the Cr, Mo, and W reaction products with CH_4 under identical experimental conditions are compared in Figure 15. Laser-ablated Cr, Mo, and W atoms are sufficiently energetic to overcome the activation energy for C−H insertion.[29] Chromium gives a single product (labeled I), which increases on visible and UV irradiation, but Mo and W form three products, which are interconverted by persistent reversible visible and UV photochemical processes, as described by Cho et al.[40] The single chromium product is CH_3−CrH, and CH_2=CrH_2 is too high in energy to form in these experiments: we note that very few chromium

(72) Cho, H.-G.; Andrews, L. Submitted for publication in *J. Phys. Chem. A* (group 6 + CH_3X).

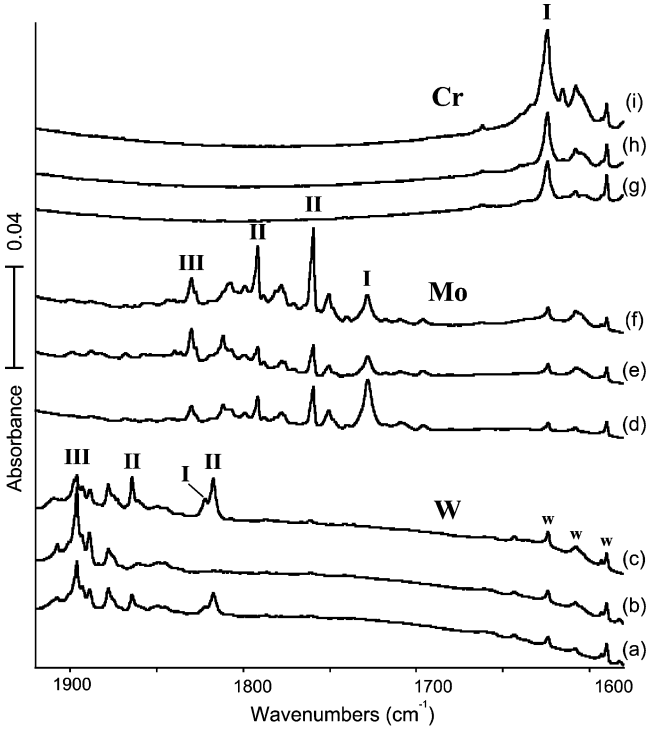

Figure 15

Figure 15. Infrared spectra in the M−H stretching region for the products of group 6 metal atom reactions with 2% methane in argon deposited at 7 K for 1 h: (a) for W; (b) after visible irradiation (>530 nm); (c) after UV irradiation (240−380 nm); (d) for Mo; (e) after visible irradiation; (f) after UV irradiation; (g) for Cr; (h) after visible irradiation; (i) after UV irradiation.

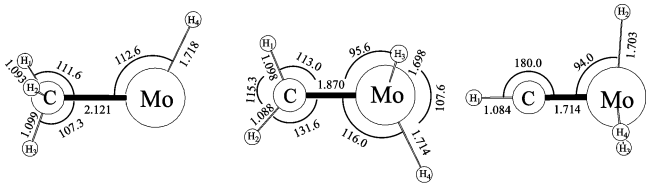

Figure 16. Structures calculated for Mo hydride, methylidene, and methylidyne complexes at the B3LYP/6-311++G(3df,3pd) level of theory (SDD for Mo). Bond lengths are given in angstroms and angles in degrees.

Scheme 2

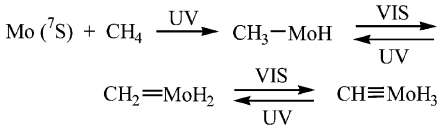

methylidene complexes are known, in contrast to the large number of Mo and W complexes.[1] The Mo case is particularly noteworthy.[38] Excited Mo activates CH_4 to give CH_3−MoH, which is characterized by a Mo−H stretching mode at 1728.0 cm^{-1} (labeled I). Visible irradiation promotes α-H transfer to give CH_2=MoH_2 with two Mo−H stretching modes at 1791.6 and 1759.6 cm^{-1} (labeled II) and a second α-H transfer to form CH≡MoH_3 with a strong MoH_3 stretching mode at 1830 cm^{-1} (labeled III). Next, UV irradiation transfers H back to carbon. These photochemical processes are completely reversible (three cycles performed), as shown by changes in the infrared spectra in Figure 15 and summarized in Scheme 2. The product identification is based on agreement between calculated and observed isotopic frequencies, as detailed previously for each

new molecule.[38] B3LYP density functional calculations show that CH≡MoH_3 has C_{3v} symmetry (Figure 16) and is a true trihydride. The Mo−H and C≡Mo stretching, MoH_2 and Mo−C−H bending, and MoH_3 rocking frequencies have also been observed for the CH≡MoH_3 methylidyne complex. A similar case has been made for CH≡WH_3.[40] We note that the C≡W stretching frequency for CH≡WH_3 in solid argon at 1003 cm^{-1} is slightly higher than the 911 cm^{-1} value reported for crystalline CH≡W$(PMe_3)_4Cl$.[73]

The C═Mo double-bond lengths computed here for CH_2═MoHF and CH_2═MoH_2 (1.838 and 1.870 Å) are in the range of X-ray diffraction values ranging from 1.827 to 1.878 Å for ligated, substituted Mo alkylidene complexes reviewed by Schrock.[1] The C≡Mo triple-bond lengths calculated for CH≡MoH_2F and CH≡MoH_3 (1.719 and 1.714 Å) are slightly shorter than the 1.743 and 1.754 Å values measured for larger $(AdO)_3$Mo≡CR complexes and the 1.762 Å value for $(R_1R_2N)_3$Mo≡$CPPh^-$. The DFT calculation of a 1.777 Å triple-bond length in the $(H_2N)_3$Mo≡$CPPh^-$ model complex[16] supports our DFT results on the simple CH≡MoH_2F and CH≡MoH_3 methylidyne complexes.[37,38] Similar agreement has been found for calculated C═W and C≡W bond lengths in the analogous simple matrix-isolated tungsten methylidene and methylidyne complexes and larger ligand-stabilized tungsten alkylidene and alkylidyne complexes.[1,39,40] The single, double, and triple carbon−tungsten bonds calculated here are slightly shorter than those measured for the [W(≡$CCMe_3$)(═$CHCMe_3$)(−CH_2CMe_3)-(dmpe)] complex.[74]

Groups 7−9

We have shown that the agostic interaction increases for CH_2═MHF complexes in the order M = Y, Zr, Nb, and Mo but reverses from CH_2═ZrH_2 to CH_2═MoH_2. Will later transition-metal atoms support α-H transfer to form methylidene complexes? Ligand-stabilized Re complexes have been prepared, and some of these are active for the metatheses of olefins.[1] Recall that early work with Mn and Fe in pure solid methane gave the insertion products CH_3−MH on photoexcitation of the metal but no evidence of α-H transfer to form methylidenes.[25] Accordingly, we investigated Mn reactions with CH_4 and CH_3F, and both gave IR spectra for the CH_3−MnH and CH_3−MnF insertion products, but no new Mn−H absorptions were observed to suggest α-H transfer to form methylidene products.[44]

In the CH_4 case, several points are noteworthy. Our major Mn−H stretching absorption at 1616.5 cm^{-1} in solid argon increased twofold on UV irradiation, and this band is 33.9 cm^{-1} higher than the analogous absorption observed at 1582.6 cm^{-1} in solid methane.[25] Clearly, the pure methane environment interacts more strongly with the presumably ^6X ground-state CH_3−MnH complex. Furthermore, the Mn−H absorption for the divalent CH_3−MnH hydride at 1616.5 cm^{-1} is just above the antisymmetric stretching frequency for MnH_2 ($^2A_1$ state, 1592.3 cm^{-1}) and substantially higher than the MnH diatomic species (1477.9 cm^{-1}).[74] The MnH and MnD diatomic molecules were also detected in these experiments. Three other modes are also observed for CH_3−MnH, methyl deformations at 1148.6 cm^{-1} and splitting at 545.2, 540.9 cm^{-1} and mostly C−Mn stretching at 505.9 cm^{-1}, which are near the pure methane values. These assignments are substantiated by isotopic substitution ($^{13}CH_4$ at 1616.5, 1140.4, 541.8, 537.7, 493.5 cm^{-1}; CD_4 at 1162.9, 892.1, 464.5 cm^{-1}; CH_2D_2 at 1615.9, 1158.3, 509.5, 1164.2, 948.2, 450.0 cm^{-1}). Note from the two products CHD_2−MnH and CH_2D−MnD formed with CH_2D_2 that there is a small amount of C−H and Mn−H mode coupling. In the CH_3F case the strong Mn−F stretching mode at 635.0 cm^{-1} shifted only slightly on isotopic substitution (633.5 cm^{-1} for $^{13}CH_3$−MnF and 628.3 cm^{-1} for CD_3−MnF).[44]

For good measure we reacted Re and CH_3F and produced CH_3−ReF, as evidenced by the Re−F stretching mode at 632.4 cm^{-1} (631.9 cm^{-1} for $^{13}CH_3$−ReF and 620.7 cm^{-1} for CD_3−ReF). We found no Re−H absorptions[75] and conclude that CH_2═ReHF was not formed in these experiments.[44]

Laser-ablated Ru was reacted with CH_4 in excess argon, and sharp new bands at 1696.0, 1684.8 cm^{-1} (1229.5, 1222.7 cm^{-1} with CD_4) increased on visible irradiation and decreased on UV irradiation, while a 1797.5 cm^{-1} absorption increased (1297.2 cm^{-1} with CD_4).[44] The former pair of bands is below the diatomic RuH band at 1820 cm^{-1} observed in previous work[76] and is in good agreement with the calculated strongest absorption (1765 cm^{-1}) for CH_3−RuH. The 1797.5 cm^{-1} band will be considered for a methylidene type complex in future work.

Finally, experiments were performed for CH_3F and Rh, and a new absorption at 559.9 cm^{-1} increased 2-fold on >290 nm and 380−240 nm irradiation, as did the CD_3F counterpart at 552.8 cm^{-1}. However, no other product absorptions were observed.[44] We assign these absorptions to the strong Rh−F stretching modes of CH_3−RhF and CD_3−RhF and conclude that CH_2═RhHF could not be formed in these experiments. Preliminary DFT calculations on CH_2═RhH_2 find little agostic distortion and 23 kcal/mol higher energy than CH_3−RhH, which may account for the failure to observe CH_2═RhH_2 in recent matrix-isolation experiments.[28]

Lanthanides and Actinides

Since the lanthanide and actinide metals fall between groups 3 and 4 in the periodic table, in a sense, Ce and Th are related to group 4, and therefore we thought that analogous hydride and methylidene complexes could be prepared with these early lanthanide and actinide metals. Substituted alkylidene complexes have not yet been synthesized with f-block elements,[77−79] although agostic Ln- - -H−C interactions have been reported for lanthanide neopentoxide complexes in the solid state and in solution.[80]

Thorium experiments were done first with methane, and a group of five bands (1435.7, 1397.1 cm^{-1} ThH_2 stretch, 670.8 cm^{-1} C═Th stretch, 634.6 cm^{-1} CH_2 wag, and 458.7 cm^{-1} ThH_2 bend) were assigned to CH_2═ThH_2 on the basis of excellent agreement with calculated frequencies.[46] The computed structure (Figure 9) reveals agostic distortion comparable to that calculated for CH_2═HfH_2. The methyl halide series of reaction products was also investigated, and the computed CH_2═ThHX structures reveal the now-established small increase in agostic distortion with increasing halogen size while the single Th−H stretching frequency increased (1380.5 to 1401.7 to 1409.5 cm^{-1}).[47]

(73) Manna, J. Kuk, R. J.; Dallinger, R. F.; Hopkins, M. D. *J. Am. Chem. Soc.* **1994**, *116*, 9793.
(74) Churchill, M. R.; Youngs, W. J. *Inorg. Chem.* **1979**, *18*, 2454.
(75) Wang, X.; Andrews, L. *J. Phys. Chem. A* **2003**, *107*, 4081.
(76) Wang, X.; Andrews, L. *J. Phys. Chem. A* **2000**, *104*, 9892.
(77) Cramer, R. E.; Maynard, R. B.; Paw, J. C.; Gilje, J. W. *J. Am. Chem. Soc.* **1981**, *103*, 3589.
(78) Pool, J. A.; Scott, B. L.; Kiplinger, J. L. *J. Am. Chem. Soc.* **2005**, *127*, 1338.
(79) Burns, C. J. *Science* **2005**, *309*, 1823.
(80) Barnhart, D. M.; Clark, D. L.; Gordon, J. C.; Huffman, J. C.; Watkin, J. G.; Zwick, B. D. *J. Am. Chem. Soc.* **1993**, *115*, 8461.

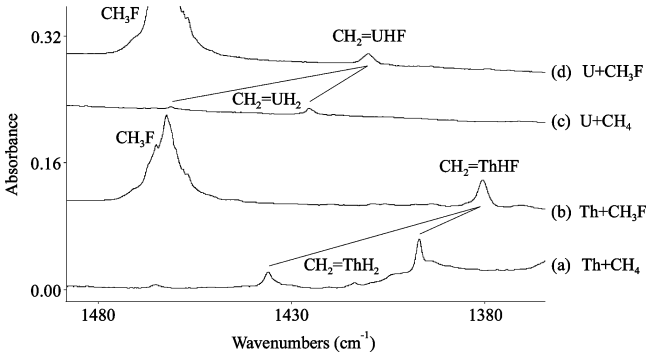

Figure 17. Infrared spectra in the M−H stretching region for products of actinide metal reactions with methane and methyl fluoride in excess argon under comparable experimental conditions (after full UV irradiation and annealing to 32−35 K): (a) Th and 5% CH_4; (b) Th and 0.5% CH_3F; (c) U and 2.5% CH_4; (d) U and 0.5% CH_3F.

Analogous reactions were also performed for uranium, and similar IR spectra were observed for the CH_2═UHX complexes.[48] The U−H stretching mode for CH_2═UHF (1410.4 cm^{-1}) is higher than that for CH_2═ThHF (1380.5 cm^{-1}), just as bands for molecular uranium hydride species are higher than those for their thorium counterparts.[81,82] Calculations for triplet ground-state CH_2═UHF are complicated by multireference character, but distorted agostic structures were found at the DFT level, which show more distortion than the thorium counterpart. IR spectra for the U and Th reaction products with CH_4 and CH_3F are compared in Figure 17. The two weak U−H stretching frequencies observed at 1461 and 1425 cm^{-1} for the U and methane reaction product bear the same relationship to the 1410.5 cm^{-1} band for CH_2═UHF that the two ThH_2 stretching modes for CH_2═ThH_2 do to the 1380.5 cm^{-1} band for CH_2═ThHF. The straightforward assignment of the new 1461 and 1425 cm^{-1} bands is to CH_2═UH_2. DFT, SOCI, and CASPT2 calculations on this uranium methylidene dihydride complex in the triplet ground state currently under investigation support this assignment.[49]

The cerium reaction with methane gives a weak 1266.8 cm^{-1} band (907.7 cm^{-1} with CD_4) that increases on UV irradiation, but no such product is apparent with neodymium. The 1266.8 cm^{-1} band is assigned to the Ce−H stretching mode of CH_3−CeH. Both Ce and Nd appear to be less reactive with CH_4 than Th and U, respectively. Cerium activation for CH_3F gives evidence for both CH_3−CeF and CH_2═CeHF, and the latter absorption at 1282.0 cm^{-1} shifts to 917.7 cm^{-1} with CD_3F. Evidence for both CH_3−NdF and CH_2═NdHF has been obtained in ongoing work. On the basis of M−H stretching absorption band intensities in comparable experiments, Ce and Nd appear to be as reactive with CH_3F as Th, but more reactive than U under similar experimental conditions. Note also that the actinide−hydrogen stretching frequencies are higher than those of their corresponding lanthanide−hydrogen counterparts in the periodic table. This arises from the effect of relativity on the heavier metals.[83] Finally, the structures calculated for CH_2═CeH_2 and CH_2═CeHF, using the same methods employed for CH_2═ThH_2 and CH_2═ThHF, respectively, reveal slightly smaller agostic H′−C−M bond angles and shorter C═M bond lengths for the lanthanide than the actinide species, and the agostic angles for the Ce species are close to the values for the analogous Ti methylidenes.[45,47]

Naked metal atom reactions with methane and methyl halides in excess argon enable synthetic chemistry in the absence of bulky stabilizing ligands. Although this methodology followed the synthetic alkylidene chemistry of Groups 4−6,[1] we have prepared the first actinide and lanthanide methylidene complexes using argon matrix reactions, and perhaps this work will stimulate further traditional synthetic efforts to prepare alkylidene complexes with actinide and lanthanide metals.

Conclusions

Several conclusions can be drawn from these experimental and theoretical investigations of transition-metal atom reactions with methane and methyl halides.

(1) The early transition, lanthanide, and actinide metal atoms react, when electronically excited, and activate methane to form insertion CH_3−MH methylmetal hydride complexes and methyl halides to form insertion CH_3−MX metal methyl halide complexes.

(2) These insertion complexes for group 3 support α-H transfer to form CH_2−MH_2 and CH_2−MHX radicals with no evidence for agostic distortion. The initial group 4−6 transition-metal insertion complexes (except for V and Cr) undergo α-H transfer to form CH_2═MH_2 or CH_2═MHX methylidene complexes, which exhibit agostic distortion. These processes are photochemically reversible in the Ti, Mo, and W systems. Group 7−9 insertion products do not sustain α-H transfer to form methylidenes, with the possible exception of Ru. The Ce, Nd, Th, and U insertion products undergo α-H transfer to form stable methylidene complexes with agostic distortion.

(3) The Mo and W methylidene complexes support a second α-H transfer and produce methylidyne complexes in reversible photochemical processes. The methylidene complexes of Nb and Ta capture electrons and undergo α-H transfer to yield the stable isoelectronic methylidyne anion complexes.

(4) Density functional theory calculations of vibrational frequencies and isotopic shifts match experimental observations and confirm the identification of new reactive molecular species. Calculated structures for different metals and halogen substituents reveal periodic trends in distortion due to agostic interactions and help characterize the electronic reorganization and structural relaxation that constitute the agostic interaction.

Acknowledgment is made to the National Science Foundation and the donors of the Petroleum Research Fund, administered by the American Chemical Society, for support of this research. We also thank J. Grunenberg for kindly providing Figure 10.

Supporting Information Available: Table S1, giving observed and calculated fundamental frequencies of CH_2═TiHI in the ground $^1A'$ electronic state. This material is available free of charge via the Internet at http://pubs.acs.org.

OM060318L

(81) Souter, P. F.; Kushto, G. P.; Andrews, L.; Neurock, M. *J. Phys. Chem. A* **1997**, *101*, 1287 (Th + H_2).

(82) Souter, P. F.; Kushto, G. P.; Andrews, L.; Neurock, M. *J. Am. Chem. Soc.* **1997**, *119*, 1682 (U + H_2).

(83) Pyykko, P. *Chem. Rev.* **1988**, *88*, 563.